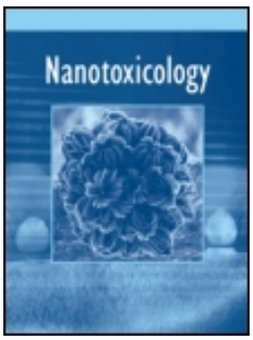

Nanotoxicology

ISSN: 1743-5390 (Print) 1743-5404 (Online) Journal homepage: https://www.tandfonline.com/loi/inan20

Titanium dioxide nanoparticles exhibit genotoxicity and impair DNA repair activity in A549 cells

Mary-Line Jugan, Sabrina Barillet, Angelique Simon-Deckers, Nathalie Herlin-Boime, Sylvie Sauvaigo, Thierry Douki & Marie Carriere

To cite this article: Mary-Line Jugan, Sabrina Barillet, Angelique Simon-Deckers, Nathalie Herlin-Boime, Sylvie Sauvaigo, Thierry Douki & Marie Carriere (2012) Titanium dioxide nanoparticles exhibit genotoxicity and impair DNA repair activity in A549 cells, Nanotoxicology, 6:5, 501-513, DOI: 10.3109/17435390.2011.587903

To link to this article: https://doi.org/10.3109/17435390.2011.587903

Nanotoxicology, August 2012; 6(5): 501–513

informa
healthcare

Titanium dioxide nanoparticles exhibit genotoxicity and impair DNA repair activity in A549 cells

MARY-LINE JUGAN[1], SABRINA BARILLET[1], ANGELIQUE SIMON-DECKERS[1], NATHALIE HERLIN-BOIME[2], SYLVIE SAUVAIGO[3], THIERRY DOUKI[3], & MARIE CARRIERE[1,3]

[1]*UMR3299 CEA-CNRS, Service Interdisciplinaire des Systèmes Moléculaires et Matériaux, Laboratoire Structure et Dynamique par Résonance Magnétique, CEA Saclay, Gif sur Yvette,* [2]*URA2453 CEA-CNRS, Service des Photons, Atomes et Molécules, Laboratoire Francis Perrin (LFP), CEA Saclay, Gif sur Yvette, and* [3]*CEA, INAC, SCIB, UJF & CNRS, LCIB (UMR_E 3 CEA-UJF and FRE 3200), Laboratoire Lésions des Acides Nucléiques, Grenoble Cedex 9, France*

(Received 20 December 2010; accepted 26 April 2011)

Abstract

Titanium dioxide nanoparticles (TiO_2-NPs) are produced in large quantities, raising concerns about their impact for human health. The aim of this study was to deeply characterize TiO_2-NPs genotoxic potential to lung cells, and to link genotoxicity to physicochemical characteristics, e.g., size, specific surface area, crystalline phase. A549 cells were exposed to a panel of TiO_2-NPs with diameters ranging from 12 to 140 nm, either anatase or rutile. A set of complementary techniques (comet and micronucleus assays, gamma-H2AX immunostaining, 8-oxoGuanine analysis, H2-DCFDA, glutathione content, antioxidant enzymes activities) allowed us to demonstrate that small and spherical TiO_2-NPs, both anatase and rutile, induce single-strand breaks and oxidative lesions to DNA, together with a general oxidative stress. Additionally we show that these NPs impair cell ability to repair DNA, by inactivation of both NER and BER pathways. This study thus confirms the genotoxic potential of TiO_2-NPs, which may preclude their mutagenicity and carcinogenicity.

Keywords: *Titanium dioxide, nanoparticle, genotoxicity, oxidative stress, DNA repair*

Introduction

Titanium dioxide nanoparticles are produced in large quantities and are already used in the production of paints, paper, and plastics as well as additives in food, cosmetics and medicines. This intensive production raises concerns about their impact for human health. Several reports address their toxicity and biodistribution, both *in vivo* and *in vitro*. The results are often controversial, but the general view is that these NPs do not cause severe lethality (Johnston et al. 2010). For the majority of toxicological endpoints tested to date, the action of TiO_2-NPs has been demonstrated to be mainly indirect, triggered by NP-induced reactive oxygen species (ROS) and reactive nitrogen species (RNS). For instance, it has been recently demonstrated that TiO_2-NPs cause apoptotic cell death and inflammation *in vitro*, which were linked to the intracellular overproduction of ROS (Hussain et al. 2009, 2010; Liu et al. 2010). Several studies have investigated TiO_2-NPs genotoxicity and cell transformation potential. Some articles show that acute *in vitro* exposure to TiO_2-NPs cause DNA strand breaks (Gurr et al. 2005; Wang et al. 2007; Kang et al. 2008; Falck et al. 2009), oxidized DNA bases (Gurr et al. 2005) and chromosomal damage as revealed by both the micronucleus assay (Rahman et al. 2002; Wang et al. 2007) and sister chromatid exchange (Lu et al. 1998). Long-term exposure to TiO_2-NPs has been shown to induce chromosomal instability and cell transformation, both *in vitro* (Huang et al. 2009) and *in vivo* (Trouiller et al.

Correspondence: Marie Carrière, presently at: CEA, INAC, SCIB, UJF & CNRS, LCIB (UMR-E3 CEA-UJF and FRE 3200), Laboratoire Lésions des Acides Nucléiques, 17 rue des Martyrs, F-38054 Grenoble Cedex 9, France. Tel: +33 4 38 78 03 28. Fax: +33 4 38 78 50 90. E-mail: marie.carriere@cea.fr

ISSN 1743-5390 print/ISSN 1743-5404 online © 2012 Informa UK, Ltd.
DOI: 10.3109/17435390.2011.587903

2009). The mechanism of TiO_2-NPs-induced genotoxicity is still under investigation. Direct interaction between NPs and DNA has been proposed on the basis of the observation of the nuclear penetration of some NPs (Chen and von Mikecz 2005). A link with induction of DNA damage and subsequent consequences remains yet to be shown. NPs may also damage DNA indirectly through induction of oxidative stress resulting of the production of ROS through chemical processes and/or inflammatory response (for review, see Schins and Knaapen 2007). In contrast to these data suggesting a significant genotoxic potential of TiO_2-NPs, other authors show that acute exposure to TiO_2-NPs do not cause DNA damage (Bhattacharya et al. 2009; Hackenberg et al. 2010). This discrepancy may be explained by differences in physicochemical properties of TiO_2-NPs suspensions, i.e., different NP diameter, crystalline phase, and/or specific surface area, or different agglomeration status. It may also be explained by the use of different cell lines that may differ in terms of susceptibility to TiO_2 toxic potential.

In an effort to understand the influence of TiO_2-NPs physicochemical characteristics on their cellular impact, we previously addressed cytotoxicity and intracellular accumulation of a panel of TiO_2-NPs in pulmonary A549 cells. This cell line was selected because exposure to NPs by inhalation and accumulation in the lung is one of the most likely risk, for instance in occupational settings. We studied TiO_2-NPs with diameters ranging from 12 to 140 nm and of anatase or rutile crystalline phases.

In this previous article, we reported that the smallest, spherically-shaped and anatase TiO_2-NPs exerted more pronounced toxic effects than rutile, elongated and larger TiO_2-NPs, even though all the tested TiO_2-NPs were accumulated in A549 cells (Simon-Deckers et al. 2008). In the present article, we focus on the evaluation of genotoxic potential of the same panel of TiO_2-NPs. The formation of DNA damage was studied through complementary techniques, including the comet assay, cytokinesis-blocked micronucleus assay, γ-H2AX histone immunostaining and 8-oxo-7,8-dihydro-2′-deoxyguanosine (8-oxodGuo) measurement. The results were then linked to some of the physicochemical characteristics of NPs. We also addressed for the first time the question of the impact of NPs exposure on the cellular DNA repair capacities. For this purpose, we used a novel multiplexed excision/synthesis assay that was recently developed by Millau et al. (2008). The bulk of our experiments show that some TiO_2-NPs may simultaneously damage DNA and decrease its repair, which could preclude deleterious events such as mutagenesis.

Materials and methods

Chemicals and nanopowders

Chemicals and cell culture media were obtained from Sigma-Aldrich. As described elsewhere (Pignon et al. 2008; Simon-Deckers et al. 2008), TiO_2-A12 and TiO_2-R20 NPs were synthesized by laser pyrolysis (Pignon et al. 2008), and annealed under air (400°C, 3 h) to remove carbon-based impurities. TiO_2-A25 (AEROXIDE® P25) were from Degussa; TiO_2-R68 (ref. 637262) and TiO_2-A140 (ref. T8141) were from Sigma-Aldrich. Their specific surface areas (SSA, m^2/g) were measured according to Brunauer Emmett and Teller (BET) protocol (Brunauer et al. 1938) on a Micromeritics Flowsorb II. Their crystalline phase was identified by X-ray powder diffraction. Particles diameters were calculated from their SSA values, as $D = 6\,000/(\rho \times SSA)$, where D is BET diameter (nm), and $\rho = 3.9$ g.cm^{-3} is the density of anatase TiO_2. Shape and primary diameter of NPs were determined by transmission electron microscopy (TEM), using a Philips EM208 microscope at 80 kV (CCME Orsay, France) by direct observation of an air-dried drop of suspension. Dimensions were measured on 150–200 randomly chosen nanoparticles. In the denomination of TiO_2-NPs used in this article, A stands for anatase, R for rutile; and the number gives the mean diameter of NP. For example TiO_2-A12 is an anatase TiO_2 NP, with a mean diameter of 12 nm.

Nanoparticles dispersion and characterization

Nanoparticles were dispersed in ultrapure sterile water (pH 5.5) by sonication for 30 min at 4°C, in pulsed mode (1 s on/1 s off), at the concentration of 10 mg.ml^{-1} (Autotune 750 W, Bioblock Scientific, operated at 28% of amplitude) (Simon-Deckers et al. 2008). The hydrodynamic diameter and zeta potentials were measured on a ZetaSizer 3000HS (Malvern, Worcestershire, UK) by photon correlation spectroscopy (PCS) and zetametry. The pH value at their zero point of charge (PZC) was obtained from their zeta potential as function of pH, thanks to a MPT-1 titrator. Just before cell exposure, suspensions were diluted in cell culture medium. Nanoparticles agglomeration state was then investigated by PCS (Malvern Zetasizer).

Cell culture

A549 human lung carcinoma cells (CCL-185) were purchased from ATCC. Cells were subcultured in DMEM containing 4.5 g.l^{-1} glucose supplemented with 2 mM L-glutamine, penicillin/streptomycin

(50 IU.mL^{-1} and 50 μg.ml^{-1}, respectively) and 10% (vol/vol) fetal bovine serum (FBS). They were maintained at 37°C in a 5% CO_2/air incubator and passed at confluence.

Cytotoxicity and intracellular internalization

Cytotoxicity was assessed by using the 3-[4,5-dimethylthiazol-2-yl]-2,5-diphenyl tetrazolium bromide (MTT) assay (Mosmann 1983). Mitochondrial succinic dehydrogenase of viable cells reduces MTT to water-insoluble blue formazan crystals which are then solubilized by dimethyl sulfoxide (DMSO); this assay thus indicates cell mitochondrial activity impairment. Cells were grown to sub-confluence in 96-well plates before being exposed to 100 μL of 1–200 μg.ml^{-1} of NP suspensions for 4–48 h (see Figure captions for details). After exposure, 10 μL of a 5 mg.ml^{-1} MTT solution were added to each well. After 1 h at 37°C, medium was then replaced by 100 μL of DMSO and mixed thoroughly to dissolve the formazan crystals. To limit potential problems due to the possible presence of residual NPs that could interfere with the assay, after addition of DMSO in the wells, NPs were allowed to sediment during 1 h and 50 μL of each well were then transferred to another plate. Then, absorbance was measured at 570 nm and cell viability was then determined as a percentage of the negative control (unexposed cells).

Colony formation ability assay was performed as follows. A total of 250 cells per well were seeded in six-well plates, and allowed to adhere for 16 h. Cells were then exposed to TiO_2-NPs for 48 h, then thoroughly rinsed three times with phosphate buffered saline (PBS), and cultured for 10 days to allow colony formation. Colonies were then stained with crystal violet (0.5% vol./vol.) and counted. Rinsing had no influence on colony formation. However it did not remove all the TiO_2-NPs adsorbed onto cell surface. These NPs might thus be internalized in cells during the cloning duration, which induce an additional exposure.

Transmission electron microscopic observations were carried out to study NP internalization into cells. After exposure, cells were fixed with 2.5% glutaraldehyde, post-fixed with OsO_4 and dehydrated in graded concentrations of ethanol (Strum et al. 1971) then embedded in Epon. Ultra-thin sections were cut (80 nm), counterstained with lead citrate and uranyl acetate and observed with a CM 12 Philips electron microscope at 80 kV (CCME Orsay, France).

Oxidative stress

Oxidative stress was first evaluated through measurements of intracellular ROS formation. To that purpose, the increasing fluorescence of 2′,7′-dichlorodihydrofluorescein diacetate acetyl ester (H_2DCFDA, Invitrogen) was monitored (Oyama et al. 1994). After exposure to NPs, cells were washed twice with PBS, and incubated 30 min at 37°C with 80 μM H_2DCFDA, then harvested by scraping. The fluorescence intensity was measured with excitation at 480 nm and emission at 530 nm (Molecular Devices Gemini X fluorescence spectrophotometer) and normalized with respect to the protein concentration. When normalizing with respect to cell number, the same trend was observed. Additionally TiO_2-NP exposure did not change the protein content/cell number ratio.

For the determination of the glutathione concentration, both total (GSH + GSSG) and reduced glutathione (GSH) contents were measured separately (Vandeputte et al. 1994). Cells lysates were prepared by scraping in phosphate buffer supplemented with glycerol and phenylmethanesulfonyl fluoride, frozen in liquid nitrogen then thawed at 37°C. The freezing/thawing cycle was repeated three times. Samples were then centrifuged (4°C, 15 min, 10,000 *g*) and supernatants were collected. Their protein concentration was measured for normalization purposes. Reduced glutathione (GSH) content was measured following derivatization by 5,5′-dithiobis(2-nitrobenzoic acid) (DTNB), which leads to the formation of 5-thio (2-nitrobenzoic acid) (TNB), a yellow by-product absorbing at 405 nm. The same protocol was applied to the determination of total glutathione content (GSH + GSSG), with a preliminary step of reduction of oxidized glutathione (GSSG) by glutathione reductase (GR). After addition of DTNB to cell lysates, absorbance at 405 nm was monitored during 5 min on a spectrophotometer, to determine the slope of TNB appearance curve. Both GSH and GSH + GSSG concentrations in cell lysates were then determined by comparison to GSH calibration curves.

The activities of enzymes responsible for cellular oxidative status maintenance, glutathione reductase (GR) and glutathione peroxydase (GPx), were evaluated using the same the cell lysates. Glutathione reductase catalyzes the NADPH-dependent reduction of GSSG to GSH. The oxidation of NADPH to $NADP^+$ is accompanied by a decrease in absorbance at 340 nm, which is thus directly proportional to GR activity (Carlberg et al. 1985). Glutathione peroxidase activity was measured indirectly, as described by Paglia and Valentine (1967), by a coupled reaction with GR. Oxidized glutathione (GSSG), produced upon reduction of cumene hydroperoxyde by GPx, is regenerated to its reduced form (GSH) by GR and NADPH. Glutathione peroxidase activity is thus deduced from the disappearance of NADPH, monitored at 340 nm.

Genotoxicity

Nanoparticle-induced strand breaks and alkali-labile sites were assessed through the alkaline version of comet assay (Singh et al. 1988). Microscope slides were coated with 1% normal melting point agarose (NMA) and allowed to dry. Around 10,000 cells (75 μL of each cell suspension) were mixed with 1% low melting point agarose (LMPA) and deposited over the agarose layer. Then 0.5% LMPA was dispensed on each slide and allowed to solidify on ice. The slides were immersed in cold lysis solution (2.5 M NaCl, 100 mM EDTA, 10 mM Tris, 10% DMSO, 1% Triton X-100) for 1 h at 4°C. DNA was then allowed to unwind for 30 min in alkaline electrophoresis solution (300 mM NaOH, 1 mM EDTA, pH > 13). Electrophoresis was performed in a field of 0.7 V/cm and 300 mA current for 24 min. Slides were then neutralized with 0.4 M Tris pH 7.5 and stained with 50 μL of 20 $\mu g.ml^{-1}$ ethidium bromide. At least 50 comets per slide were analyzed under a fluorescence microscope (Zeiss) equipped with a 350–390 nm excitation and 456 nm emission filter at ×20 magnification. Comet length and intensity were measured by using Comet IV software (Perceptive Instruments, Suffolk, UK).

The amount of γ-H2AX foci per cell nuclei was evaluated after a 24 h exposure to TiO_2-NPs, by immunostaining of cells fixed for 20 min in 3% paraformaldehyde, using a anti-γ-H2AX antibody (Upstate, dilution 1/500, vol./vol.). As positive control, we used A549 cells exposed to 50 μM of etoposide for 24 h. Cell nuclei were stained for 15 min with DAPI (10 $\mu g.ml^{-1}$). Total number of foci was automatically measured on images containing 50–100 cell nuclei, with ImageJ software. At least five slides and three images per slides were analyzed in each condition. Apoptotic cells and dividing cells were removed from the calculation.

The micronucleus assay was performed as described by Fenech (2000). As positive control, we used A549 cells exposed to 25 μM of etoposide for 24 h. After exposure to TiO_2-NPs for 24 h, cells were cultured another 24 h in complete medium containing 4 $\mu g.ml^{-1}$ of cytochalasin B, in order to block cytokinesis. Cells were then fixed for 20 min in 3% paraformaldehyde and stained with acridine orange (5 $\mu g.ml^{-1}$) and DAPI (10 $\mu g.ml^{-1}$). Exposure was performed in triplicate, and five pictures were taken on each slide, resulting in 15 pictures per condition. On each image, the total number of binucleated cells and the number of micronuclei were counted (i.e., approximately 1500 nuclei). These pictures contained a maximum of 2 micronuclei, micronucleus induction was thus insignificant. Consequently we did not calculate all the parameters described by Fenech (2000).

For quantification of 8-oxodGuo and other oxidized bases by HPLC-tandem mass spectrometry (HPLC-MS/MS) (Frelon et al. 2000), DNA was extracted and digested as described by Ravanat et al. (2002). Briefly, a lysis buffer containing Triton X-100 was added to the cellular pellet. The nuclei were collected by centrifugation and further lyzed in a second buffer containing 10% SDS. The sample was incubated with a mixture of RNAse A and RNAse T1, and subsequently treated by proteinase. DNA was recovered by precipitation using isopropanol and concentrated sodium iodide. Deferroxamine was added to all buffers to prevent spurious oxidation. DNA was then digested into a mixture of nucleosides first by incubation with nuclease P1, DNaseII and phosphodiesterase II at pH 6 (2 h). A second step involved alkaline phosphatase and phosphodiesterase I (2 h, pH 8). The solution was neutralized with 0.1 μM HCl and centrifuged. The supernatant was collected and injected onto the HPLC-MS/MS system. The API 3000 mass spectrometer (SCIEX) was used in the multiple reaction monitoring mode with positive electrospray ionization. The monitored fragmentation was m/z 284 $[M + H]^+ \rightarrow$ m/z 168 $[M + H - 116]^+$ for 8-oxodGuo. Chromatographic separations were achieved using a C18 reversed phase Uptisphere ODB column (Interchim, Montluçon, France). The elution was performed using a gradient of methanol in 2 mM ammonium formate at a flow rate of 0.2 $ml.min^{-1}$. The retention time was around 29 min. In addition to the MS spectrometer, the HPLC eluent was analyzed in a UV detector set at 270 nm to quantify the amount of unmodified nucleosides. Levels of 8-oxodGuo were expressed as number of lesions per million normal bases.

Activity of DNA repair enzymes

The base excision repair (BER) and nucleotide excision repair abilities (NER) of A549 cells exposed to TiO_2-NPs were assessed using the newly developed multiplexed excision/synthesis assay (Millau et al. 2008). Nuclear extracts were prepared as described in (Millau et al. 2008), and excision/repair reactions were run for 2.5 h at 30°C at a final protein concentration of 0.8 $mg.ml^{-1}$, in a medium containing 1 mM adenosine triphosphate and 1.25 μM dCTP-Cy5 (Amersham, Little Chalfont, Bucks, UK), on damaged plasmid microarrays (Millau et al. 2008). The assessed lesions were photoproducts (cyclobutane pyrimidine dimers and (6–4) photoproducts), 8-oxodGuo, alkylated bases, abasic sites, and pyrimidine glycols. For each lesion, the total fluorescence

incorporated into lesion-containing plasmid was measured (Genepix 4200A scanner, Axon GenePix, Molecular Device, Sunnyvale, CA, USA) and normalized to the fluorescence incorporated in undamaged plasmid. The experiment was reproduced three times.

Statistical analysis

Each experiment was performed at least three times. Statistical tests were run using the Statistica 7.1 software (Statsoft, Chicago, IL, USA). As normality assumptions for valid parametric analyses, even after data log transformation, were not satisfied (Kolmogorov-Smirnov tests), non-parametric one-way analyses of variance on ranks approach (Kruskal-Wallis) were used. When significance was demonstrated ($^{\star}p < 0.05$), paired comparisons were run using Mann-Whitney tests.

Results

Nanoparticle characterization, cytotoxicity and cellular internalization in A549 cells

Cells were exposed to a panel of thoroughly characterized TiO_2-NPs (Table I). Briefly TiO_2-NPs are either rutile or anatase, and their diameter range from 12–140 nm. Most of them are round-shaped, whereas TiO_2-R68 is elongated-shaped. The present results are complementary to those that we previously published (Simon-Deckers et al. 2008), and include the spherical, rutile TiO_2-R20 NP.

On the basis of a MTT assay optimized for studying the cytotoxic potential of NPs, and when data were expressed on a mass unit base, we observed that round-shaped TiO_2-NPs, both rutile and anatase, with diameters lower than 100 nm exerted more pronounced toxic effects than TiO_2-NPs with diameters higher than 100 nm (Figure 1A).

The TiO_2-NPs that induced the more pronounced cytotoxic events, i.e., TiO_2-A12, -A25 and -R20 caused less than 25% of cell death after 48 h of exposure. TiO_2-A140 and -R68 led to lethality below 10% and 1%, respectively, after 48 h of exposure. Consequently, diameter rather than crystalline phase was found to be the major parameter influencing TiO_2-NPs cytotoxic potential. The weak loss of cell viability obtained after exposure to TiO_2-R68 NPs may thus be due both to their elongated shape and to their size (their length is 68 nm). In addition, the influence of TiO_2-NPs on cell proliferation was assessed by the colony formation ability assay (Figure 1B). The number of clones tended to decrease upon exposure to TiO_2-NPs; however, it was not statistically significant.

In order to better characterize the interaction between TiO_2-NPs and cells, we used TEM to visualize putative intracellular accumulation. This analysis was performed at an early time point in order to better observe differences between the internalization kinetics of NPs with different physicochemical properties.

An unambiguous accumulation of the smallest NPs (TiO_2-A12, TiO_2-A25 and TiO_2-R20) was observed in the cytoplasms, and TiO_2-A12 was also observed in the nucleus of cells (Figure 2). For larger NPs, cytoplasmic accumulation was also observed, but NPs were never observed in cell nuclei.

Cellular oxidative status

We then evaluated intracellular ROS content in TiO_2-NPs exposed cells by using the H_2DCFDA assay. Intracellular ROS production increased significantly after a short-time exposure (4 h) of A549 cells to TiO_2-NPs, whatever their diameter, shape and crystalline phase (Figure 3A). All the NPs that were tested in our laboratory in the H_2DCFDA assay (TiO_2, Al_2O_3, SiC, SiO_2, Au, carbon nanotubes) caused an increase of intracellular ROS content (not shown). This response was thus not specific to TiO_2-NPs. We also tested the possibility that NPs would interact with

Table I. TiO_2 nanoparticles physicochemical characteristics[a].

NP	Furnisher	Shape	Crystal. phase	Diameter (nm)	SSA (m^2/g)	PZC
A12	LFP	Spherical	95% anatase	12 nm	92 m^2/g	6.4
A25	Degussa ref Aeroxide® P25	Spherical	86% anatase	24 nm	46 m^2/g	7.0
A140	Sigma ref. T8141	Spherical	100% anatase	142 nm	10 m^2/g	5.2
R68	Sigma ref. 637262	Elongated	100% rutile	L: 68 nm d: 9 nm	118 m^2/g	-
R20	LFP	Spherical	90% rutile	21 nm	73 m^2/g	nd

[a]LFP, Laboratoire Francis Perrin; L, length; d, diameter; SSA, specific surface area; PZC, point of zero charge; nd, not determined.

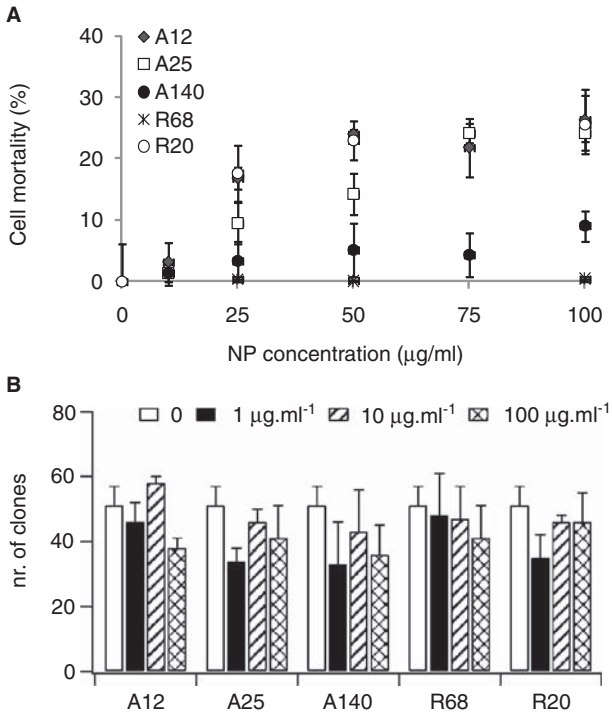

Figure 1. Cytotoxicity evaluation of TiO_2-NPs. Cellular metabolic activity impairment, reflecting cell mortality, was assessed by using the MTT assay (A). Cell mortality was also evaluated through the clonogenic assay (B). Tests were performed after a 48 h exposure to TiO_2-NPs, prepared in DMEM medium (without serum). Results are presented as mean of 8 points ± standard deviation (MTT assay) or 5 points ± standard deviation (clonogenic assay).

H_2DCFDA: In parallel to these experiments we exposed cells to TiO_2-NPs, and then followed exactly the protocol described in the *Material and methods* section, but without incubating cells with H2DCFDA. We did not observe any fluorescence, proving that TiO_2-NPs did not produce fluorescence that would lead to false positive results.

In cells exposed to A25, intracellular ROS production started as early as after 15 min of exposure, and increased until it reached a plateau, after 4 h of exposure (Figure 3B). After 24 h, intracellular ROS content remained higher in cells exposed to TiO_2-A12, -A25 and -R20 than in control (unexposed) cells (Figure 3A). Conversely, it drastically decreased in cells exposed to TiO_2-A140 or -R68, reaching the level obtained in unexposed cells.

Information on the redox status of the cells was also gathered from the determination of the intracellular content in glutathione, a major component of the antioxidant defense. Total glutathione (GSH + GSSG) and reduced glutathione (GSH) contents were measured. Generally, total glutathione (Figure 4A) and reduced glutathione (Figure 4B) contents were weakly modulated by TiO_2-NP exposure. They tended to decrease, although this decrease was not statistically significant, except upon exposure to TiO_2-R68 for 24 h (total glutathione) and to TiO_2-A12 or -R20 for 24 h (reduced glutathione).

Finally, the activities of enzymes responsible for cycling of glutathione between its reduced and oxidized form (GR and GPx) were evaluated (for a schematic representation of the enzymes implicated in cell redox status maintenance, see Barillet et al. 2010). These activities were not modified after 4 and 24 h of exposure to any of these TiO_2-NPs (Figure 5).

Damage to DNA

TiO_2-NPs impact on DNA integrity was evaluated using a panel of complementary techniques. First the alkaline single-cell electrophoresis assay (comet assay) was applied to TiO_2-NPs-exposed cells.

After 4 h of exposure, whatever the TiO_2-NPs, a significant increase in the level of DNA breaks was

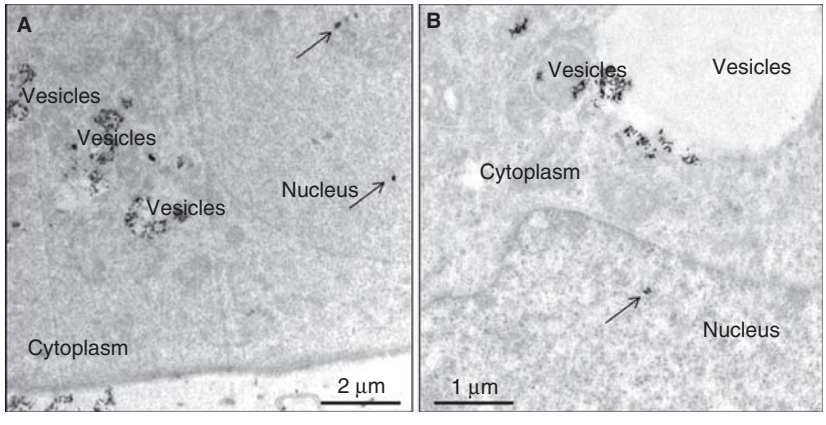

Figure 2. Intracellular accumulation of TiO_2-NPs. Cell exposed for 4 h to 50 µg.ml^{-1} of TiO_2-A12. NPs were included in Epon resin, sectioned and observed by using a transmission electron microscope (TEM). NPs are visible in cell cytoplasm (c.), trapped in vesicles (v.), or in cell nuclei (n.) (arrows).

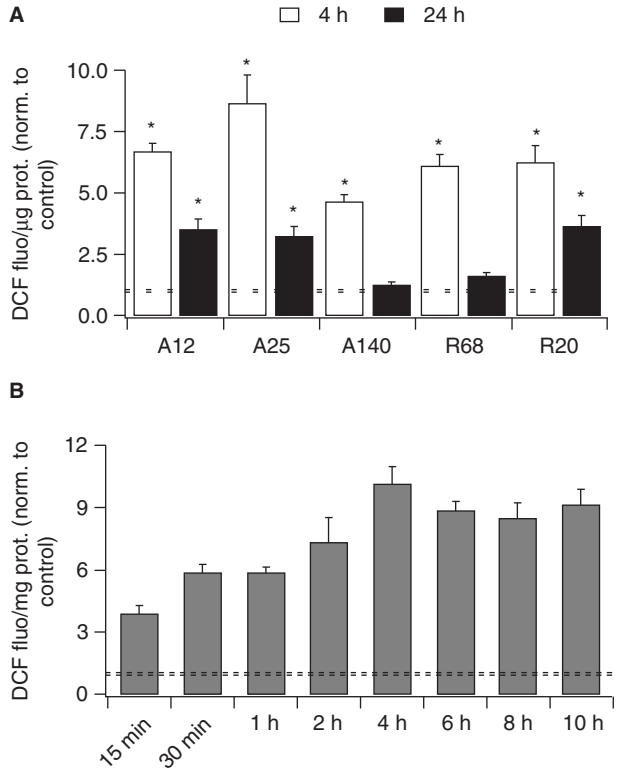

Figure 3. Intracellular ROS content. ROS content was evaluated by measurement of DCF fluorescence, after exposure of cells to 100 µg.ml^{-1}of TiO_2-NPs for 4 or 24 h and then to H2DCFDA for 30 min (A), or after exposure to 100 µg.ml^{-1}of A25-NP for 15 min–8 h and then to H2DCFDA for 30 min (B). DCF fluorescence was then normalized to protein content, reflecting cell number. For comparison purpose, the obtained data were then divided by DCF content in control samples (unexposed cells); dotted lines represent the standard deviation of control samples. Results are mean of 4 points ± standard deviation.

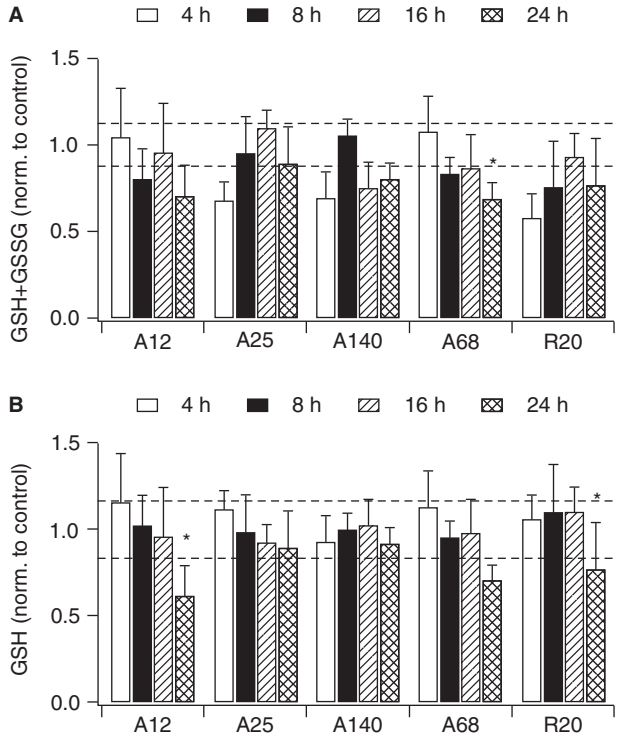

Figure 4. Glutathione content. Total (A) and reduced (B) glutathione cellular content was measured after exposure for 4, 8, 16 or 24 h to 100 µg.ml^{-1} of TiO_2-NPs. Results are expressed as percent of the negative control (unexposed cells), mean of 4 points ± standard deviation. Dotted lines represent the standard deviation of control samples.

observed (Figure 6A and Table II). This increase in the level of breaks further increased after 24 h of exposure, still it was statistically significant only after exposure to TiO_2-A12, -A25 and -R20, but not to TiO_2-R68 and -A140. After 48 h of exposure, the frequency of breaks drastically decreased in exposed cells. It reached the basal level, i.e., the level of DNA breakage observed in unexposed cells, in all samples except in cells exposed to TiO_2-A12, where a significant DNA fragmentation was still observed.

The amount of 8-oxodGuo and other oxidized bases within DNA was measured by HPLC associated with tandem mass spectrometry (HPLC-MS/MS) (Ravanat et al. 1998). This technique is one of the most sensitive and allows the detection of up to 11 oxidatively modified bases and nucleotides in cellular DNA (Cadet et al. 2010). The only oxidized base detected in TiO_2-NPs-exposed cells was 8-oxodGuo (Figure 6B). Other lesions such as thymidine glycols, 5-(hydroxymethyl)-2′-deoxyuridine, 5-formyl2-2′-deoxyuridine or 8-oxo-7,8-dihydro-2′-deoxyadenosine were either below the detection limit or were not produced in higher frequency upon treatment (data not shown). After 4 h of exposure, the level of 8-oxodGuo increased in cells exposed to TiO_2-A12 and -A25. After 24 and 48 h, their amount further increased, and also significantly increased in cells exposed to TiO_2-R20 and -R68, reaching final values of 10–15 8-oxodGuo per million of DNA bases. Since we did not use any invert particles as control, we however cannot prove that this cellular response is specific of TiO_2-NPs. Conversely, the amount of 8-oxodGuo was never higher in TiO_2-A140-exposed cells than in control cells.

The comet assay reveals both single- and double-strands breaks, but the latter are present in much lower proportion. In order to gain insight into the formation of DNA double-strand breaks, we quantified the number of γ-H2AX foci, the appearance of which is a specific and early response of cells to this type of DNA lesion (Paull et al. 2000). The recorded signal was not modified by cell exposure to TiO_2 A12 or A25, two NPs chosen for their significant genotoxic potential as observed by the comet assay (Table III). Similarly, the number of clastogenic and

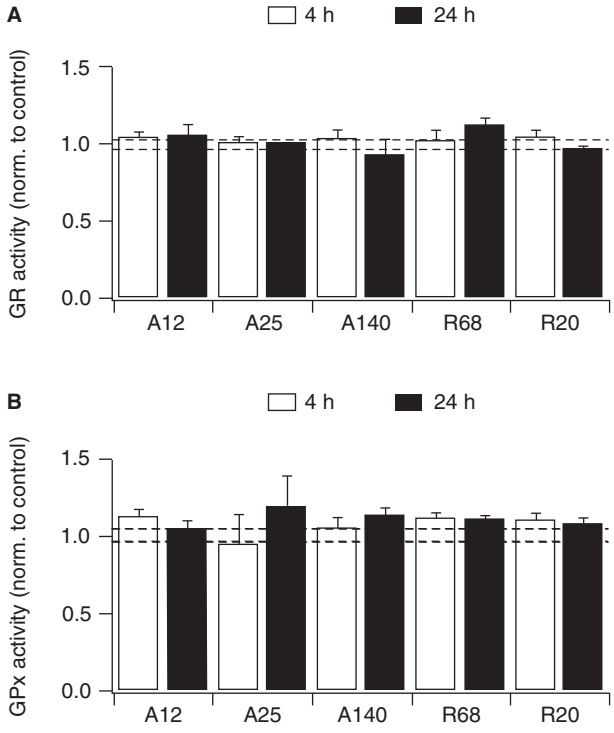

Figure 5. Antioxidant enzymes activities. Glutathion reductase (GR, A) and glutathione peroxidase (GPx, B) activities were evaluated in cells exposed for 4 and 24 h to 100 $\mu g.ml^{-1}$ of TiO_2-NPs. Results are expressed as percent of the negative control (unexposed cells), mean of 4 points ± standard deviation. Dotted lines represent the standard deviation of control samples.

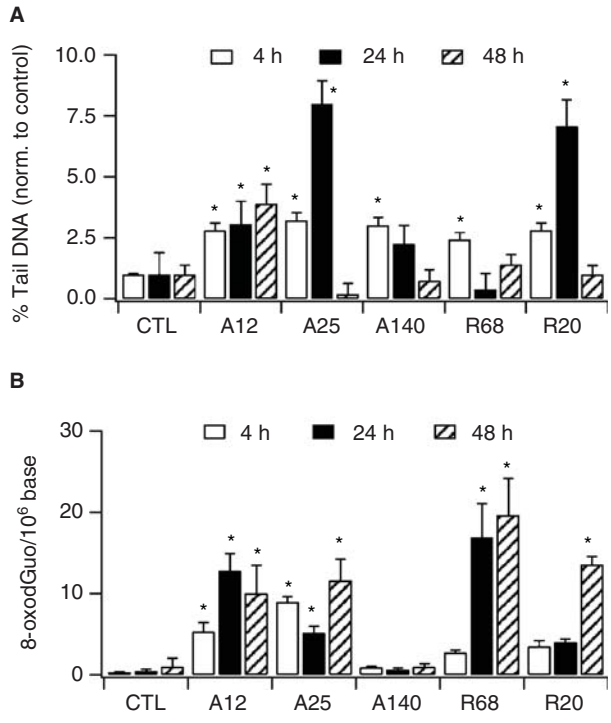

Figure 6. TiO_2-NPs genotoxicity. Genotoxicity was assessed by using the comet assay (A) and measurement of 8-oxodGuo lesions (B) after exposure for 4, 24 or 48 h to 100 $\mu g.ml^{-1}$ TiO_2-NPs. Comets were scored on at least 50 cells per slide, and 8-oxodGuo lesions were measured by HPLC-MS-MS on 10 millions of cells per sample, in triplicate. Results are presented as median of % DNA in comet tail ± standard deviation (comet assay), and number or 8-oxodGuo lesions per 10^6 bases ± standard deviation (8-oxodGuo assay).

aneugenic events did not increase (Table IV) as assessed by the cytokinesis-blocked micronucleus assay (Fenech 2000) on cells exposed to TiO_2-A12 or A25.

Cellular ability to repair DNA damage

To determine the effect of TiO_2-NPs exposure on DNA repair capacities, we performed a multiplexed excision/synthesis assay (Millau et al. 2008) on nuclear extracts of TiO_2-NPs-exposed cells. This assay evaluates the ability of cells to repair DNA lesions by both nucleotide excision repair (NER, CPD-64 and CisP) and base excision repair (BER, 8oxo, AlkB, AbaS and glycol) pathways. The assay was processed at a sublethal concentration of NPs (30% cell death at 48 h for the small NPs and below 10% for the largest ones) and with a constant concentration of nuclear proteins, ensuring that the modulation of DNA repair ability was not caused by a lower number of cells which may be due to TiO_2-NPs-induced cell death. Neither could it be caused by an unspecific adsorption of DNA repair enzymes to TiO_2-NPs, which would then be eliminated during the cell lysis steps.

Strikingly, after a 24 h exposure (Figure 7A), TiO_2-A12 and -A140 drastically decreased cellular excision/repair ability of all the tested lesions, as compared to the repair ability of unexposed cells. BER and NER pathways were inhibited to the same extent. In cells exposed to TiO_2-R68 and -R20, the inhibition was also significant, but less marked. Conversely, TiO_2-A25 slightly increased the repair ability of all the tested lesions. Maybe NP diameter should explain this difference, however other parameters are also determinant since A140 is as efficient as A12 in inhibiting DNA repair ability. After 48 h of exposure (Figure 7B), the inhibition was generalized, and even TiO_2-A25 caused the inhibition of repair ability of all the tested lesions. The more active NPs were TiO_2-A12 and -R20 at this late time point.

Discussion

In this article, we report the oxidative stress and genotoxic events caused on A549 cells by TiO_2-NPs varying in their size (12–140 nm), crystalline phase (anatase, rutile) and shape (spherical, elongated). We

Table II. % DNA in comet tail, absolute values[a].

	Ctl	A12	A25	A140	R68	R20
4 h	8.6 ± 0.4	24.0 ± 2.8	27.6 ± 2.8	25.9 ± 2.8	21.0 ± 2.5	24.1 ± 2.5
24 h	2.6 ± 2.3	7.9 ± 2.4	20.5 ± 2.5	5.8 ± 2.0	1.0 ± 1.7	18.1 ± 2.8
48 h	7.2 ± 2.7	28.0 ± 5.9	1.3 ± 3.2	5.4 ± 3.3	10.1 ± 3.0	7.1 ± 2.8

[a]% DNA in comet tail is the median of at least 50 comets per slides.

previously applied a similar strategy to evaluate their cytotoxic potential and cellular accumulation (Simon-Deckers et al. 2008), but an ambiguity remained since the only tested rutile NPs (TiO_2-R68) were elongated-shaped, while all the anatase NPs were spherical. Rutile TiO_2-NPs are generally elongated-shaped due to the crystalline arrangement of Ti and O atoms. Comparing the toxic effects of spherical anatase NPs to the toxic effect of elongated rutile NPs avoids discriminating between the influence of crystalline phase and of shape. The control of laser pyrolysis parameters permitted to obtain the spherical and rutile TiO_2-NPs, and their use in our panel of TiO_2-NPs enabled to conclude on the influence of crystalline phase and shape independently.

On all the tested endpoints (cytotoxicity, ROS production, GSH content, DNA damage as measured by comet assay and 8-oxodGuo lesions content, DNA repair ability), the most deleterious effects were found in cells exposed to TiO_2-A12, -A25 and -R20, i.e., the smallest NPs (diameter <68 nm) and the spherical ones, whatever their crystalline phase. These observations are in line with observed ability of these small NPs at accumulating inside the cells, both in the cytoplasm and the nucleus, as observed here after cell exposure for 4 h to TiO_2-A12. The influence of size on TiO_2-NPs toxicity has already been described on several endpoints (Johnston et al. 2010), but the influence of crystalline phase is less reported. Some studies show that anatase NPs induce more deleterious effects than rutile NPs, which is explained by the photocatalytic properties of anatase TiO_2 (Johnston et al. 2010). However, here, experiments have been processed in the dark to avoid any photocatalytic effect of NPs, which would generate artefactual accumulation of ROS in cells.

Table III. Gamma-H2AX foci[a].

	50 $\mu g.ml^{-1}$	100 $\mu g.ml^{-1}$	200 $\mu g.ml^{-1}$
Ctl−	9.9 ± 1.7		
Ctl+	70.0 ± 7.0		
A12	10.2 ± 0.6	8.3 ± 1.5	8.4 ± 1.5
A25	11.7 ± 2.4	12.5 ± 2.5	9.7 ± 1.2

[a]Total number of foci on a microscope slide were counted after immonostaining with γ-H2AX antibody, then total number of cell nuclei was evaluated. Ctl−: unexposed cells. Ctl+: cells exposed 24 h to 50 μM etoposide. Results are presented as the ratio of number of foci/number of cell nuclei. Cells were exposed to TiO_2-NPs for 24 h.

Our results confirm that TiO_2-NPs cause an early intracellular accumulation of ROS, which is high and statistically significant for all the tested NPs. This accumulation is transient and decreases between 4 and 24 h of exposure. In parallel, a general trend to GSH cellular content reduction after exposure to TiO_2-NPs was observed, although significantly only after exposure to the smallest and spherical ones, and after 24 h of exposure. Such a decrease suggests that this molecular antioxidant has been consumed to detoxify cells from ROS overproduction caused by TiO_2-NPs. No modification in GR activity is observed, meaning that the intracellular GSH pool is not restored from GSSG. This is in line with our observation that the total glutathione content decreases already 4 h after exposure, while the effect on reduced GSH is more pronounced at 24 h, showing that cells are not able to compensate the oxidation of GSH.

We thoroughly investigated genotoxicity, one of the most long-term deleterious effects of oxidative stress. Damage to DNA caused by TiO_2-NP exposure, *in vitro*, has already been reported in several studies (for review, see Singh et al. 2009). Among the applied techniques described in the literature, micronucleus measurements (Gurr et al. 2005; Wang et al. 2007; Falck et al. 2009; Shukla et al. 2011) and comet assay (Gurr et al. 2005; Wang et al. 2007; Falck et al. 2009; Hackenberg et al. 2010; Shukla et al. 2011) are the most employed, and lead to contradictory results: either no genotoxicity (Falck et al. 2009; Hackenberg et al. 2010), or induction of DNA damage (Gurr et al. 2005; Wang et al. 2007; Shukla et al. 2011). In an attempt to resolve these contradictory results, we extensively characterized the NPs we tested, and used a wide array of complementary approaches to evaluate their genotoxic potential. This strategy allowed us to propose that the oxidative stress associated with exposure to TiO_2-NPs induced the formation of DNA lesions and decreases the repair capacities. Indeed, we observed significant induction of DNA strand breaks visualized by the comet assay

Table IV. Micronucleus assay[a].

	50 μg.ml^{-1}		100 μg.ml^{-1}		200 μg.ml^{-1}	
	BC	MN	BC	MN	BC	MN
Ctl−	41.4 ± 2.0	0.4 ± 0.5				
Ctl+	20 ± 2.0	12 ± 1.5				
A12	21.0 ± 2.2	0.0 ± 0.0	22.6 ± 3.1	3.1 ± 1.0	23.6 ± 3.6	0.0 ± 0.0
A25	19.0 ± 3.0	0.2 ± 0.4	19.4 ± 6.1	0.0 ± 0.0	16.0 ± 4.3	0.2 ± 0.4

[a]Micronuclei (MN) were counted in binucleated cells (BC). Ctl−: unexposed cells. Ctl+: cells exposed 24 h to 25 μM etoposide. Data are presented as mean number of MN or mean number of BC per slide ± standard deviation, counted on five slides per condition. Cells were exposed to TiO_2-NPs for 24 h.

during the first 24 h of treatment. This trend was mostly observed for the spherical TiO_2-NPs with diameter smaller than 68 nm whatever their crystalline phase. In contrast, large TiO_2-NPs (68 nm, 140 nm) did not significantly increase the amount of DNA strand breaks. All parameters measured by comet assay (tail moment, tail DNA, olive tail moment...) followed the same trend. Comet assay enables detecting DNA strand breaks of oxidative origin and alkali-labile sites such as abasic sites and unstable DNA adducts (Singh et al. 1988; Tice et al. 2000). Because no organic compound was involved in our experiments, contribution of the latter class of DNA damage can be ruled out. It is also proposed that the comet assay reveals sites produced by excision repair (Alapetite et al. 1997). Yet, time-course comet analysis after exposure to genotoxic stress shows a decrease in the number of breaks rather than an increase as would be expected consecutively to DNA repair (Brammer et al. 2001; Calini et al. 2002). In addition, a number of genotoxic stresses, including UVB (Kielbassa et al. 1997), singlet oxygen (Pouget et al. 2002) or Benzo[a]pyrene (Tarantini et al. 2009) lead to repairable DNA damage with little strand breaks. It can thus be concluded that the genotoxic events revealed by comet assay measurements within this study correspond to breaks produced by ROS. The contribution of double-strand breaks to the comet assays results is negligible since no γ-H2AX was observed in treated cells. Absence of chromosomal damage was also demonstrated by the lack of positive results in the micronuclei assay.For all these assays, cells were exposed to TiO_2-NPs prepared in cell culture medium that did not contain serum, which means that cells division - and consequently DNA replication - was only a marginal event.

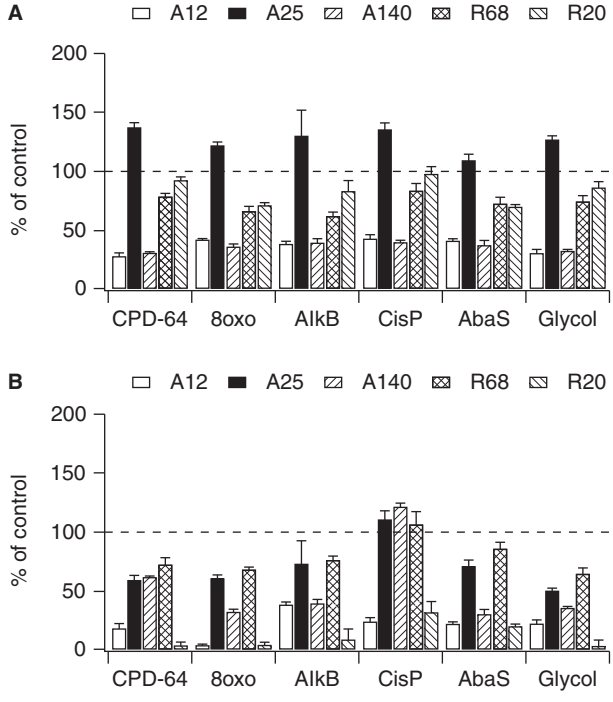

Figure 7. TiO_2-NPs impact on DNA repair ability. DNA repair activity was evaluated on nuclear lysates of cells exposed to 100 μg.ml^{-1} of TiO_2-NPs for 24 h (A) or 48 h (B), using DNA repair microarray. Results are means of three spots ± standard deviation, the experiment was performed three times.

Evidence for the induction of oxidative damage to DNA was also gained from the measurement of the level of 8-oxodGuo. Indirect evidence for the formation of the mutagenic oxidized base has been reported by others, using the comet assay involving conversion of oxidized purine bases into additional breaks by the Fpg bacterial DNA repair enzyme (Gurr et al. 2005). In order to obtain more specific information, we determined the level of 8-oxodGuo lesions and concluded that TiO_2-NP exposure lead to their accumulation, in rather high amounts as compared to other genotoxic stress at equal cytotoxicity (Douki et al. 1999). Only the large anatase NP left the level of 8-oxodGuo unchanged.

Comparison of the time-dependence on the induction of DNA damage may provide information on the nature of the involved ROS. The observation of DNA strand breaks induction within the first 24 h of

exposure shows that hydroxyl radicals (°OH) are produced. Indeed, they are the only ROS able to attack the DNA backbone (Pogozelski and Tullius 1998). In cells, °OH is likely produced through Fenton processes, namely the reaction of hydrogen peroxide (H_2O_2) with metal ions. Ti is not a precursor of Fenton reactions and the tested TiO_2-NPs do not contain any metallic impurities (Simon-Deckers et al. 2008). Hydroxyl radicals thus probably occur by reaction between hydrogen peroxide and cellular endogenous metal ions. This is consistent with the results of the H2DCFDA experiments, this probe being mostly sensitive to H_2O_2. Note that °OH is so reactive that it does not diffuse in cells. Accordingly, strand breaks were produced mostly by the small TiO_2-NPs, which were shown by us and others (Chen and von Mikecz 2005) to accumulate in the nuclei. It is thus consistent with an intranuclear production of H_2O_2 triggered by NPs accumulated in cell nuclei, further reacting with metals to form °OH, which locally induce DNA breaks. In contrast to strand breaks, 8-oxodGuo is generally produced in cells by all types of oxidant (Cadet et al. 2010). It is thus not surprising that NPs inducing little strand breaks, such as R68, efficiently oxidize guanine. Such a result means that weaker oxidizing species than hydroxyl radicals (e.g., hydroperoxides) are produced by all the tested NPs. This could also explain why damage arising from oxidation of the other bases was not observed. Similarly, the observation that the level of 8-oxodGuo remains elevated longer than that of strand breaks could be explained by a change in the nature of the oxidative stress with time, for instance as the results of the modification of chemical composition of the NP surface.

Alternative explanations to the time-course formation of the different types of DNA damage can be found. First, the rapid decrease in the level of DNA strand breaks between 24 and 48 h could be explained by the elimination of cells containing the most altered DNA. However, cells were exposed at TiO_2-NP concentrations leading to less than 30% of cell mortality; we thus rather thought that the observed effect was more due to DNA repair. Decrease in break frequency would be explained by the end of their formation associated to an efficient repair. As far as 8-oxodGuo is concerned, the longer persistence of this oxidized base with respect to breaks could also be explained by the decrease in DNA repair capacities induced by NPs.

Indeed, we observed that exposure to TiO_2-NPs drastically impaired cellular DNA repair through both the NER and BER pathways. Although some actors of DNA repair are involved in both BER and NER, these two pathways are quite independent. A parallel inhibition of NER and BER is striking, and reveals that NPs impact the upstream and early steps of DNA repair processes. A hypothesis may be that TiO_2-NPs impair DNA lesions detection by the cellular machinery. Defective DNA repair may also result from impaired recruitment and activity of DNA repair proteins. It may be proposed that protein inactivation results from their structural modification, for instance by oxidation which may be caused by TiO_2-NPs-induced ROS accumulation. Indeed, protein oxidation/reduction is regarded as a critical mechanism for the modulation of their activity (Bravard et al. 2009). DNA repair proteins then have to recognize the damaged site, then to combine to form the appropriate DNA repair complex. This complex then tailors DNA gap and finally promotes the synthesis of the proper DNA sequence and the ligation of this sequence to the undamaged DNA backbone. These steps of DNA repair processes may probably be less affected by TiO_2-NPs, since the effectors involved in NER and BER pathways are different. More experiments are needed to identify the central(s) step(s) involved in this cellular response.

Conclusions

The present study confirms that TiO_2-NPs cause an oxidative stress and exhibit genotoxicity to A549 cells, the smallest and spherical NPs exerting the more pronounced toxic effects, independently of their crystalline phase. Oxidative DNA damage, including single-strand breaks and 8-oxodGuo, but not double-strand breaks or chromosomal breaks or losses, was produced. We also observed, for the first time, that these NPs impair cell ability to repair damage to DNA, by inactivation of both NER and BER pathways. This combination of induction of DNA damage and decrease in the cellular capacities to respond to this genotoxic stress can be seen as synergistic deleterious effects, on the way to mutagenesis and carcinogenesis upon exposure to TiO_2-NPs. Obviously, our results were obtained on cultured cells with rather large amounts of NPs and remain to be confirmed *in vivo*.

Acknowledgement

The authors would like to thank D. Jaillard from CCME Orsay, France, for her help in transmission electron microscopy experiments, and S. Caillat from LAN, for his help in multiplexed DNA repair assays.

Declaration of interest: This study was funded by the French national research agency through the 2007-SEST-021 grant, by the ANSES through

EST-0802 grant, and by CEA through internal Toxicology and Technology for health programs. The authors report no conflicts of interest. The authors alone are responsible for the content and writing of the paper.

References

Alapetite C, Benoit A, Moustacchi E, Sarasin A. 1997. The comet assay as a repair test for prenatal diagnosis of Xeroderma pigmentosum and trichothiodystrophy. J Investigat Dermatol 108:154–159.

Barillet S, Jugan M-L, Laye M, Leconte Y, Herlin-Boime N, Reynaud C, Carrière M. 2010. In vitro evaluation of SiC nanoparticles impact on A549 pulmonary cells: Cyto-, genotoxicity and oxidative stress. Toxicol Lett 198(3):324–330.

Bhattacharya K, Davoren M, Boertz J, Schins RPF, Hoffmann E, Dopp E. 2009. Titanium dioxide nanoparticles induce oxidative stress and DNA-adduct formation but not DNA-breakage in human lung cells. Part Fibre Toxicol 6(17).

Brammer I, Zoller M, Dikomey E. 2001. Relationship between cellular radiosensitivity and DNA damage measured by comet assay in human normal, NBS and AT fibroblasts. Int J Radiat Biol 77:929–938.

Bravard A, Vacher M, Moritz E, Vaslin L, Hall J, Epe B, Radicella JP. 2009. Oxidation status of human OGG1-S326C polymorphic variant determines cellular DNA repair capacity. Cancer Res 69(8):3642–3649.

Brunauer S, Emmett PH, Teller E. 1938. Adsorption of gases in multimolecular layers. J Am Chem Soc 60(2):309–319.

Cadet J, Douki T, Ravanat J-L. 2010. Oxidatively generated base damage to cellular DNA. Free Rad Biol Med 49(1):9–21.

Calini V, Urani C, Camatini M. 2002. Comet assay evaluation of DNA single- and double-strand breaks induction and repair in C3H10T1/2 cells. Cell Biol Toxicol 18:369–379.

Carlberg I, Mannervik B, Alton M. 1985. Glutathione reductase. Meth Enzymol 113:484–490.

Chen M, von Mikecz A. 2005. Formation of nucleoplasmic protein aggregates impairs nuclear function in response to SiO_2 nanoparticles. Experim Cell Res 305(1):51–62.

Douki T, Perdiz D, Grof P, Kuluncsics Z, Moustacchi E, Cadet J, Sage E. 1999. Oxidation of guanine in cellular DNA by solar UV radiation: Biological role. Photochem Photobiol 70(2):184–190.

Falck GCM, Lindberg HK, Suhonen S, Vippola M, Vanhala E, Catalan J, Savolainen K, Norppa H. 2009. Genotoxic effects of nanosized and fine TiO_2. Human Experim Toxicol 28(6–7): 339–352.

Fenech M. 2000. The *in vitro* micronucleus technique. Mutat Res 455(1–2):81–95.

Frelon S, Douki T, Ravanat JL, Pouget JP, Tornabene C, Cadet J. 2000. High-performance liquid chromatography-tandem mass spectrometry measurement of radiation-induced base damage to isolated and cellular DNA. Chem Res Toxicol 13(10):1002–1010.

Gurr JR, Wang ASS, Chen CH, Jan KY. 2005. Ultrafine titanium dioxide particles in the absence of photoactivation can induce oxidative damage to human bronchial epithelial cells. Toxicology 213(1–2):66–73.

Hackenberg S, Friehs G, Froelich K, Ginzkey C, Koehler C, Scherzed A, Burghartz M, Hagen R, Kleinsasser N. 2010. Intracellular distribution, geno- and cytotoxic effects of nanosized titanium dioxide particles in the anatase crystal phase on human nasal mucosa cells. Toxicol Lett 195(1):9–14.

Huang S, Chueh PJ, Lin Y-W, Shih T-S, Chuang S-M. 2009. Disturbed mitotic progression and genome segregation are involved in cell transformation mediated by nano-TiO_2 long-term exposure. Toxicol Appl Pharmacol 241(2):182–194.

Hussain S, Boland S, Baeza-Squiban A, Hamel R, Thomassen LCJ, Martens JA, Billon-Galland MA, Fleury-Feith J, Moisan F, Pairon JC, Marano F. 2009. Oxidative stress and proinflammatory effects of carbon black and titanium dioxide nanoparticles: Role of particle surface area and internalized amount. Toxicology 260(1–3):142–149.

Hussain S, Thomassen LCJ, Ferecatu I, Borot MC, Andreau K, Martens JA, Fleury J, Baeza-Squiban A, Marano F, Boland S. 2010. Carbon black and titanium dioxide nanoparticles elicit distinct apoptotic pathways in bronchial epithelial cells. Part Fibre Toxicol 7(10).

Johnston HJ, Hutchison GR, Christensen FM, Peters S, Hankin S, Stone V. 2010. Identification of the mechanisms that drive the toxicity of TiO_2 particulates: The contribution of physicochemical characteristics. Part Fibre Toxicol 6(33).

Kang SJ, Kim BM, Lee YJ, Chung HW. 2008. Titanium dioxide nanoparticles trigger p53-mediated damage response in peripheral blood lymphocytes. Environ Molec Mutagen 49(5): 399–405.

Kielbassa C, Roza L, Epe B. 1997. Wavelength dependence of oxidative DNA damage induced by UV and visible light. Carcinogenesis 18:811–816.

Liu SC, Xu LJ, Zhang T, Ren GG, Yang Z. 2010. Oxidative stress and apoptosis induced by nanosized titanium dioxide in PC12 cells. Toxicology 267(1–3):172–177.

Lu PJ, Ho IC, Lee TC. 1998. Induction of sister chromatid exchanges and micronuclei by titanium dioxide in Chinese hamster ovary-K1 cells. Mutat Res 414(1–3):15–20.

Millau JF, Raffin AL, Caillat S, Claudet C, Arras G, Ugolin N, Douki T, Ravanat JL, Breton J, Oddos T, Dumontet C, Sarasin A, Chevillard S, Favier A, Sauvaigo S. 2008. A microarray to measure repair of damaged plasmids by cell lysates. Lab Chip 8(10):1713–1722.

Mosmann T. 1983. Rapid colorimetric assay for cellular growth and survival: Application to proliferation and cytotoxicity assays. J Immunolog Meth 65(1–2):55–63.

Oyama Y, Hayashi A, Ueha T, Maekawa K. 1994. Characterization of 2′,7′-dichlorofluorescin fluorescence in dissociated mammalian brain neurons: Estimation on intracellular content of hydrogen peroxide. Brain Res 635(1–2):113–117.

Paglia DE, Valentine WN. 1967. Studies on quantitative and qulitative characterization of erythrocyte glutathione peroxidase. J Lab Clin Med 70(1):158.

Paull TT, Rogakou EP, Yamazaki V, Kirchgessner CU, Gellert M, Bonner WM. 2000. A critical role for histone H2AX in recruitment of repair factors to nuclear foci after DNA damage. Curr Biol 10(15):886–895.

Pignon B, Maskrot H, Leconte Y, Coste S, Reynaud C, Herlin-Boime N, Gervais M, Guyot Ferreol V, Pouget T, Tranchant JF. 2008. Versatility of laser pyrolysis applied to synthesis of TiO_2 nanoparticles, application to UV attenuation. Eur J Inorgan Chem 6:883–889.

Pogozelski WK, Tullius TD. 1998. Oxidative strand scission of nucleic acids: Routes initiated by hydrogen abstraction from the sugar moiety. Chem Rev 98(3):1089–1107.

Pouget J-P, Frelon S, Ravanat J-L, Testard I, Odin F, Cadet J. 2002. Formation of modified bases in cells exposed either to gamma radiation or high-LET particles. Radiat Res 157:589–595.

Rahman Q, Lohani M, Dopp E, Pemsel H, Jonas L, Weiss DG, Schiffmann D. 2002. Evidence that ultrafine titanium dioxide

induces micronuclei and apoptosis in Syrian hamster embryo fibroblasts. Environ Health Perspect 110(8):797–800.

Ravanat JL, Douki T, Duez P, Gremaud E, Herbert K, Hofer T, Lasserre L, Saint-Pierre C, Favier A, Cadet J. 2002. Cellular background level of 8-oxo-7,8-dihydro-2′-deoxyguanosine: An isotope based method to evaluate artefactual oxidation of DNA during its extraction and subsequent work-up. Carcinogenesis 23(11):1911–1918.

Ravanat JL, Duretz B, Guiller A, Douki T, Cadet J. 1998. Isotope dilution high-performance liquid chromatography – electrospray tandem mass spectrometry assay for the measurement of 8-oxo-7,8-dihydro-2′-deoxyguanosine in biological samples. J Chromatogr B –Analyt Technol Biomed Life Sci 715:349–356.

Schins RPF, Knaapen AM. 2007. Genotoxicity of poorly soluble particles. Inhalat Toxicol 19:189–198.

Shukla RK, Sharma V, Pandey AK, Singh S, Sultana S, Dhawan A. 2011. ROS-mediated genotoxicity induced by titanium dioxide nanoparticles in human epidermal cells. Toxicol vitro 25(1):231–241.

Simon-Deckers A, Gouget B, Mayne-L'hermite M, Herlin-Boime N, Reynaud C, Carriere M. 2008. *In vitro* investigation of oxide nanoparticle and carbon nanotube toxicity and intracellular accumulation in A549 human pneumocytes. Toxicology 253(1–3):137–146.

Singh N, Manshian B, Jenkins GJS, Griffiths SM, Williams PM, Maffeis TGG, Wright CJ, Doak SH. 2009. NanoGenotoxicology: The DNA damaging potential of engineered nanomaterials. Biomaterials 30(23–24):3891–3914.

Singh NP, McCoy MT, Tice RR, Schneider EL. 1988. A simple technique for quantitation of low levels of DNA damage in individual cells. Experim Cell Res 175(1):184–191.

Strum JM, Wicken J, Stanbury JR, Karnovsky MJ. 1971. Appearance and function of endogenous peroxidase in fetal rat thyroid. J Cell Biol 51(1):162–175.

Tarantini A, Maitre A, Lefebvre E, Marques M, Marie C, Ravanat JL, Douki T. 2009. Relative contribution of DNA strand breaks and DNA adducts to the genotoxicity of benzo[a] pyrene as a pure compound and in complex mixtures. Mutat Res 671(1–2):67–75.

Tice RR, Agurell E, Anderson D, Burlinson B, Hartmann A, Kobayashi H, Miyamae Y, Rojas E, Ryu JC, Sasaki YF. 2000. Single cell gel/comet assay: Guidelines for *in vitro* and *in vivo* genetic toxicology testing. Environ Molec Mutagen 35(3): 206–221.

Trouiller B, Reliene R, Westbrook A, Solaimani P, Schiestl RH. 2009. Titanium dioxide nanoparticles induce DNA damage and genetic instability *in vivo* in mice. Cancer Res 69(22):8784–8789.

Vandeputte C, Guizon I, Genestie-Denis I, Vannier B, Lorenzon G. 1994. A microtiter plate assay for total glutathione and glutathione disulfide contents in cultured/isolated cells: Performance study of a new miniaturized protocol. Cell Biol Toxicol 10(5–6):415–421.

Wang JJ, Sanderson BJS, Wang H. 2007. Cyto- and genotoxicity of ultrafine TiO_2 particles in cultured human lymphoblastoid cells. Mutat Res 628(2):99–106.